

See discussions, stats, and author profiles for this publication at: <https://www.researchgate.net/publication/231640197>

# Vector–Algebra Approach To Obtain Molecular Fields from Conical Intersections: Numerical Applications to $H + H_2$ and $Na + H_2^+$

ARTICLE in THE JOURNAL OF PHYSICAL CHEMISTRY A · MAY 2004

Impact Factor: 2.69 · DOI: 10.1021/jp049706w

CITATIONS

3

READS

14

## 5 AUTHORS, INCLUDING:



Ágnes vibók

University of Debrecen

103 PUBLICATIONS 1,116 CITATIONS

SEE PROFILE



Tamas Vertesi

Hungarian Academy of Sciences

81 PUBLICATIONS 822 CITATIONS

SEE PROFILE



Erika Bene

Hungarian Academy of Sciences

18 PUBLICATIONS 124 CITATIONS

SEE PROFILE



Michael Baer

Hebrew University of Jerusalem

345 PUBLICATIONS 8,033 CITATIONS

SEE PROFILE

# Vector–Algebra Approach To Obtain Molecular Fields from Conical Intersections: Numerical Applications to $\text{H} + \text{H}_2$ and $\text{Na} + \text{H}_2^\dagger$

Á. Vibók,<sup>‡</sup> T. Vértési,<sup>‡</sup> E. Bene,<sup>§</sup> G. J. Halász,<sup>||</sup> and M. Baer<sup>\*,‡,⊥</sup>

Department of Theoretical Physics, University of Debrecen, Debrecen, Hungary, Institute of Chemistry, Chemical Research Center, Hungarian Academy of Sciences, Budapest, Hungary, and Institute of Informatics, University of Debrecen, Debrecen, Hungary

Received: January 20, 2004; In Final Form: April 17, 2004

In this paper is presented a theory according to which *all* of the elements of the nonadiabatic coupling matrix,  $\tau_{jk}(q, \varphi)$ , are created at the *singular* points of the system. (These points are known also as points of conical intersections.) For this purpose, we consider the angular distribution of the angular components,  $\tau_{qjk}(q_j \sim 0, \varphi_j)$ , at the close vicinity of their singularities, namely, around the  $j$ th singularity points  $q_j = 0$ . It is shown that these distributions determine the intensity of the entire field created by the nonadiabatic coupling matrix at every point in the region of interest. To support these statements, the three lower states of the  $\text{H} + \text{H}_2$  system (which in our example form three conical intersections) and the third and fourth states of the  $\text{Na} + \text{H}_2$  system (which in our example form four conical intersections) are considered. From ab initio treatments, we obtain the above-mentioned angular distributions and, having those, create the field at every desired point employing vector–algebra. The final results are compared with ab initio calculations.

## I. Introduction

This paper is part of a collection of papers to honor our friend and colleague Professor Gert D. Billing. What makes this paper somewhat special is the fact that the subject considered here was started together with Professor Billing (and Professor John Avery) while one of the authors (M.B.) spent part of his Sabbatical at the Department of Chemistry at the University of Copenhagen.<sup>1,2</sup>

In recent years, efforts were invested to study the nature of the electronic nonadiabatic coupling terms (NACTs).<sup>3–11</sup> The NACTs are characterized by two features: They are vectors<sup>12,13</sup> (in contrast to potentials that are scalars), and they may become singular<sup>14</sup> (in contrast to potentials that do not). If arranged in matrices, they acquire a third interesting feature, namely, that the matrices are antisymmetric.

Because NACTs follow from the Born–Oppenheimer treatment<sup>12</sup> and because they appear in the nuclear Schrödinger equation that follows, they are on the same footing as the potential energy surfaces. Therefore, so it seems, the ordinary way to get acquainted with the NACTs is to study their spatial structure—somewhat reminiscent of the way potential energy surfaces are studied—and then eventually to apply them. However, as it turns out, this idea is somewhat naive because the *singularity* of the NACTs adds a new *dimension* in the study of molecular processes. Being singular hints toward the possibility that the NACTs are a kind of field that has its origin at these singular points,<sup>1,2,15</sup> which produce nonlocal effects. In what follows, this field is termed as the *molecular field*. The intriguing idea to categorize the singularity points of the NACTs

as sources for a field is somewhat reminiscent of the fields produced by charged particles (electrons, protons, etc.) and the spatial distribution of the NACTs as the spatial intensity of the field. The aim of this paper is to show, by applying ab initio calculations, that a theory of this kind is plausible.

Although we mentioned charges as possible sources for a field, the sources for the present (molecular) field are not electric charges. As is now known, the NACTs fulfill (extended) Curl equations<sup>13</sup> and therefore have their origin, just like the electromagnetic vector potential, in magnitudes that are pseudo magnetic fields. This possibility becomes most apparent when considering two isolated states that form a (single) singularity. Such an analysis performed a few years ago shows that the two-state NACT,  $\boldsymbol{\tau}$  (see below for proper definitions), can be simulated as a vector potential formed by an infinitely long and narrow solenoid. In other words,  $\boldsymbol{\tau}$  was assumed to fulfill the equation<sup>15</sup>

$$\text{Curl } \boldsymbol{\tau} = \mathbf{H} \quad (1)$$

where  $\mathbf{H}$  is modeled as a (pseudo) magnetic field produced by an “electric current” along a solenoid. Because  $\mathbf{H}$  is nonzero only inside the solenoid and because the solenoid is very narrow, it can be, mathematically, presented as

$$\mathbf{H} = 2\pi f(\varphi) \frac{\delta(q)}{q} \quad (2)$$

where  $(q, \varphi)$  are polar coordinates in a plane perpendicular to the solenoid,  $\delta(q)$  is the Dirac delta function, and  $f(\varphi)$  is some function of the angle  $\varphi$  chosen in such a way as to satisfy certain features, as will be discussed below.

The fact that  $\boldsymbol{\tau}$  fulfills eq 1 implies, semiclassically, that it results from a quasi-electric current that flows along the solenoid. The solenoid according to the model is formed from a line of degeneracy points known by the name *seam*. In what follows, we term the degeneracy points as points of conical

<sup>†</sup> Part of the “Gert D. Billing Memorial Issue”.

\* Corresponding author. Permanent address: Soreq Nuclear Research Center, Yavne 81800, Israel. E-mail: michaelb@fh.huji.ac.il.

<sup>‡</sup> Department of Theoretical Physics, University of Debrecen.

<sup>§</sup> Hungarian Academy of Sciences.

<sup>||</sup> Institute of Informatics, University of Debrecen.

<sup>⊥</sup> Szent-Györgyi Albert Professor.

intersection and use the acronym ci (see refs 16 and 17 for detailed studies regarding the ci's and their importance for solid-state physics and molecular physics).

As long as our system behaves as a two-state Hilbert subspace, the above equations are fulfilled and the relevant theory follows accordingly (see also the next section). However, in general, the two-state approximation soon breaks down, and as a result, the ordinary Curl equation has to be replaced by a more general equation, the extended Curl equation, which, among other things, contains nonlinear terms.<sup>13</sup> In what follows, we discuss this extension for three states and employ ab initio results to study its relevance.

The Hilbert subspace, in a given region, is formed from a group of states where each *adjacent* pair forms one (or several) ci(s).<sup>18</sup> According to its definition, a Hilbert subspace *cannot* contain two adjacent states that do not form at least one ci. In other words, adjacent states that do not form a ci with states within the subspace are excluded. Nonadjacent states (e.g., the first and third) usually do not form a ci, but this by no means implies that the corresponding NACT (in this particular example,  $\tau_{13}$ ) is identically zero. This subject is discussed extensively in the third section.

## II. Theory

**II.1. Introductory Remarks.** The magnitudes to be discussed in the present paper are  $\tau_{qjk}/q$ , the angular component of  $\tau$ , and  $\tau_{qjk}$ , the radial component, both defined as<sup>12</sup>

$$\tau_{\lambda jk} = \left\langle \zeta_j \left| \frac{\partial}{\partial \lambda} \right| \zeta_k \right\rangle; \quad \lambda = q, \varphi; \quad j (\neq k) = \{1, \dots, N\} \quad (3)$$

where  $q$  and  $\varphi$  are the two corresponding (nuclear) polar coordinates in the plane of interest and the  $|\zeta_k(s_e|q, \varphi)\rangle$  functions are the eigenfunctions of an electronic Hamiltonian  $\mathbf{H}_e(s_e|q, \varphi)$ :

$$[\mathbf{H}_e(s_e|q, \varphi) - u_k(q, \varphi)]|\zeta_k(s_e|q, \varphi)\rangle = 0; \quad k = 1, \dots, N \quad (4)$$

Here  $u_k(q, \varphi)$  is the  $k$ th electronic eigenvalue and  $s_e$  stands for the electronic coordinate.

A few decades ago, it was verified that any system of electronic eigenfunctions that forms a Hilbert space and for any pair of Cartesian nuclear coordinates  $(x, y)$  the corresponding NACT matrices fulfill the following equation:<sup>13</sup>

$$\mathbf{F}_{xy} = \frac{\partial \tau_y}{\partial x} - \frac{\partial \tau_x}{\partial y} - [\tau_y, \tau_x] = 0 \quad (5)$$

known as the extended Curl equation (to distinguish it from the ordinary Maxwellian Curl equation). In the present paper, we consider only two (polar) coordinates, and in this case, eq 5 reduces to

$$\tilde{\mathbf{F}}_{q\varphi} = \frac{1}{q} \left( \frac{\partial \tau_\varphi}{\partial q} - \frac{\partial \tau_q}{\partial \varphi} - [\tau_q, \tau_\varphi] \right) = 0 \quad (6)$$

This equation was proved to exist, *approximately*, also for a group of states that forms a Hilbert subspace at a given region.<sup>18b</sup> The Curl equation (as well as the extended version) is discussed frequently in the literature and will not be elaborated in this article.<sup>6,7,19</sup> Equation 6, as applied for a Hilbert subspace, is one of the subjects in the present study.

**II.2. Treatment of the Two-State System in a Plane. II.2.1. General Theory.** In the case of a subspace of two states, the

commutator in eq 6 becomes zero so that the equation reduces to the more familiar form

$$\text{Curl } \tau = 0 \quad (6')$$

where  $\tau$ , in this case, is a  $2 \times 2$  vector matrix of the form

$$\tau = \begin{pmatrix} 0 & \tau \\ -\tau & 0 \end{pmatrix} \quad (7)$$

It is noticed that, in this case, the  $\tau$  matrix contains only one nonzero term,  $\tau$ , and therefore the Curl equation for the matrix  $\tau$  becomes the Curl equation for this matrix element  $\tau = (\tau_q, \tau_\varphi/q)$

$$\text{Curl } \tau = \frac{1}{q} \left( \frac{\partial \tau_\varphi}{\partial q} - \frac{\partial \tau_q}{\partial \varphi} \right) = 0 \quad (8)$$

Equation 8 is valid at every point except at the singularity point. To include this point (assuming we have only one point like this), eq 8 is extended to become (see also eq 1)

$$\frac{\partial \tau_\varphi}{\partial q} - \frac{\partial \tau_q}{\partial \varphi} = 2f(q) \delta(q) \quad (9)$$

In what follows, we consider  $\tau_\varphi$  as the only unknown function (thus, we ignore the fact that  $\tau_q$  is also unknown), so that its solution can be shown to be (by substitution)

$$\tau_\varphi(q, \varphi) - \int_0^q dq \frac{\partial \tau_q}{\partial \varphi} = h(q) f(\varphi) \quad (10)$$

where  $h(q)$  is the Heaviside function. Because  $q$  is always positive,  $h(q)$  can be ignored and eq 10 becomes

$$\tau_\varphi(q, \varphi) - \int_0^q dq \frac{\partial \tau_q}{\partial \varphi} = f(\varphi) \quad (11)$$

To determine  $f(\varphi)$ , we consider eq 11 in the limit of  $q \rightarrow 0$ . From numerous ab initio calculations, it is verified that  $\tau_q$  in the interval  $q \sim 0$  is finite and therefore

$$f(\varphi) = \tau_\varphi(q \sim 0, \varphi) \quad (12)$$

Because  $\tau_\varphi$  is known to be quantized (reminiscent of the Bohr–Sommerfeld quantization but applied to a spin), we have a similar quantization for  $f(\varphi)$ :<sup>20</sup>

$$\int_0^{2\pi} \tau_\varphi(q, \varphi) d\varphi = n\pi \rightarrow \int_0^{2\pi} f(\varphi) d\varphi = n\pi \quad (13)$$

In what follows (and because of eq 12),  $f(\varphi)$  is defined as the *virgin* angular component related to a given ci. The reason being that usually any part of a NACT is affected by neighboring NACTs, except for a section located at an *infinitely* small region surrounding its own ci.

So far, we discussed only  $\tau_\varphi(q \sim 0, \varphi) [=f(\varphi)]$ . As for  $\tau_q$ , the situation is somewhat different. Numerical studies show that  $\tau_q(q)$  is finite as  $q \rightarrow 0$ <sup>21</sup> and therefore is orders of magnitude smaller than  $\tau_\varphi(q)/q$  (in this region). Because a single ci for the two-state Hilbert subspace is rare if it exists at all, it is not clear whether the nonzero  $\tau_q$  values in the close vicinity of  $q \sim 0$  that are obtained by the ab initio calculation are essentially produced by other ci's or by the ci under consideration. Therefore, in what follows, we assume that the *virgin* radial component,  $\tau_q(q, \varphi)$ , is always identically zero.

The situation in the close vicinity of each ci is summarized as follows:

$$\tau(q \sim 0, \varphi) = \{\tau_\varphi(q \sim 0, \varphi)/q, \tau_q(q \sim 0, \varphi)\} = \{f(\varphi)/q, 0\} \quad (14)$$

The rest is just algebra.

Before completing this section, we return to eq 2 in order to make a connection between the findings regarding  $f(\varphi)$  and the pseudo magnetic field  $\mathbf{H}$  along the seam. Because  $f(\varphi)$  is quantized, this implies that  $\mathbf{H}$  is quantized as well. In other words, the quantization we encounter for  $\tau$  has its origin in the quantization of the pseudo magnetic field that exists along the seam. This situation, which is reminiscent of Dirac's quantization of the magnetic monopole, was discussed, to some extent, in ref 15.

**II.2.2. Application of Vector–Algebra To Form the Two-State Molecular Field.** In the previous section, we analyzed a system with a single ci (see eq 14). Next we consider the situation where the two states form several ci's. In this case, just like in electrodynamics, vector–algebra is employed to add up the contributions of the various ci's to obtain the resultant intensity of the field at a given point.

For this purpose, we first derive the mathematical expression for the field due to a ci located at an arbitrary point  $(q_{j0}, \varphi_{j0})$ . The procedure is as follows: Having  $\tau = [f_j(\varphi_j)/q_j, 0]$ , we present it in terms of *Cartesian* components  $(\tau_x, \tau_y)$  and then shift the solution to the point of interest, namely,  $(0, 0) \rightarrow (x_{j0}, y_{j0}) [= (q_{j0}, \varphi_{j0})]$ . Once completed, the solution is transformed back to polar coordinates. The derivation, presented elsewhere, yields for a given point  $P(q, \varphi)$  (as measured from the new origin) the following results:<sup>1,2</sup>

$$\begin{aligned} \tau_q(q, \varphi) &= -f_j(\varphi_j) \frac{1}{q_j} \sin(\varphi - \varphi_j) \\ \tau_\varphi(q, \varphi) &= f_j(\varphi_j) \frac{q}{q_j} \cos(\varphi - \varphi_j) \end{aligned} \quad (15)$$

where the connection between the various coordinates is as follows:

$$\begin{aligned} q_j &= \sqrt{(q \cos \varphi - q_{j0} \cos \varphi_{j0})^2 + (q \sin \varphi - q_{j0} \sin \varphi_{j0})^2} \\ \cos \varphi_j &= \frac{q \cos \varphi - q_{j0} \cos \varphi_{j0}}{q_j} \end{aligned} \quad (16)$$

It is noticed that for  $q_{j0} \rightarrow 0$  (and therefore  $\varphi_j \rightarrow \varphi$ ) the solution in eq 15 yields  $[\tau_\varphi(q, \varphi)/q, \tau_q(q, \varphi)] \equiv [f_j(\varphi_j)/q, \tau_q \rightarrow 0]$ , which is the solution for the case where the ci is at the origin. A similar situation is encountered as  $q \gg q_{j0}$ . Here, too,  $\varphi_j \rightarrow \varphi$  and therefore  $\tau_q \rightarrow 0$ .

We attached to each ci a different  $f(\varphi)$  function, i.e.,  $f_j(\varphi_j)$ , to indicate that each such ci (in this case the  $j$ th one) may form a different virgin distribution.

With this modified expression, we can now extend the solution of eq 15 to any number of ci's. Because  $\tau_\varphi(q, \varphi)$  and  $\tau_q(q, \varphi)$  are scalars, the solution in the case of  $N$  ci's is obtained by summing up the contributions of all ci's:<sup>1,2</sup>

$$\tau_q(q, \varphi) = -\sum_{j=1}^N f_j(\varphi_j) \frac{1}{q_j} \sin(\varphi - \varphi_j)$$

$$\tau_\varphi(q, \varphi) = q \sum_{j=1}^N f_j(\varphi_j) \frac{1}{q_j} \cos(\varphi - \varphi_j) \quad (17)$$

Equation 17 yields the two components of  $\tau(q, \varphi)$  for a distribution of two-state ci's expressed in terms of the *virgin* distributions of the NACTs at their ci's. These functions have to be obtained from ab initio treatments; however, the entire field is formed by eq 17.

**II.3. Treatment of the Three-State System in a Plane.** The three-state  $\tau$  matrix is given in the form

$$\tau = \begin{pmatrix} 0 & \tau_{12} & \tau_{13} \\ -\tau_{12} & 0 & \tau_{23} \\ -\tau_{13} & -\tau_{23} & 0 \end{pmatrix} \quad (18)$$

and the corresponding three-state Curl equations become<sup>2</sup>

$$\text{Curl } \tau_{12} = [\tau_{23} \times \tau_{13}] \quad (19a)$$

$$\text{Curl } \tau_{23} = [\tau_{13} \times \tau_{12}] \quad (19b)$$

$$\text{Curl } \tau_{13} = [\tau_{12} \times \tau_{23}] \quad (19c)$$

As is noticed, the extension from two states to three states is much more involved than just adding another equation. Comparing eq 19 with eq 6' (or with eq 8) shows already some of the difficulties with this extension. In the two-state case, all we have to do is employ vector–algebra to obtain the components of  $\tau$ , but no differential equations have to be solved. In the three-state system, the vector–algebra may at most yield a first guess for the inhomogeneity terms related to the Curl equations of the various  $\tau$  matrix elements, but then to obtain the  $\tau$  elements themselves, one is forced to solve differential equations. Moreover, these differential equations are nonlinear, which may introduce additional complications.

The three equations in eq 19 contain six unknown functions, namely,  $(\tau_{qjk}, \tau_{qjk})$ ;  $k > j, j = 1, 2$ . Thus, to solve them, we need to find another three equations (this subject was recently discussed in refs 21 and 22). The present paper differs from the ones just mentioned by the fact that these (differential) equations will not be solved. Here we only apply vector–algebra to validate the relevance of the equations themselves.

Before we start with the numerical part, we discuss an important feature given in eq 19. We argued on several occasions that singularities can be formed only between two adjacent states and therefore only the NACTs;  $\tau_{ij+1}$  values are formed by their own singularities, whereas the other NACTs, of the kind  $\tau_{jk}$  ( $k \neq j + 1$ ), have to be formed in a different way. Equation 19c implies that such a NACT, namely,  $\tau_{13}$ , is formed by the mutual interaction of the first two NACTs,  $\tau_{12}$  and  $\tau_{23}$ . If these two NACTs do not interact, namely, do not overlap in the region of interest,  $\tau_{13}$  becomes identically zero in that region. This finding can be expressed in a different way: If  $\tau_{13}$  is zero at every point in the region of interest, then the two first equations become decoupled, and as a result, the assumed three-state Hilbert subspace breaks up into two two-state Hilbert subspaces: one subspace between the two lower states and one subspace between the two upper spaces. In other words, having two groups of ci's—one group that couples the two lower states and one group that couples the two upper states—does not necessarily guarantee that the three states form a real three-state Hilbert space.

The case in which  $\tau_{13}$  is zero at every point in the region of interest has also practical implications because in this situation



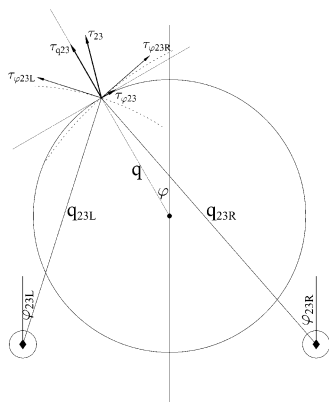


**Figure 1.** Schematic figure to show the various vectors due to two sources (ci's) for constructing the  $\varphi$  and  $q$  components of  $\tau(\varphi|q)$ , the NACT along a circle centered at an arbitrary point. Around each (the  $j$ th) source is drawn an infinitesimal circle along which are given the ab initio (undisturbed) values of  $\tau_{\varphi j}(\varphi_j|q_j \sim 0) = f_j(\varphi_j)$ .

the calculation of  $\tau_{12}$  and  $\tau_{23}$  will be carried out, independently, using, as before, vector–algebra only.

### III. Numerical Results

This section is divided into two parts: In the first part, we show to what extent the straightforward vector–algebra is capable of producing the two-state NACTs. This treatment will be carried out for two systems: (a) for the two upper states (the second and third) of the  $\text{H} + \text{H}_2$  system [in this case are encountered two ci's, and we sum up the components of the two respective NACTs (employing eq 17) and compare the results with ab initio calculations] and (b) for the third and the fourth states of the  $\text{Na} + \text{H}_2$  system [in this case we have four ci's and, again, we sum up the components of all of them and compare with ab initio calculations].

In the second part, we discuss some aspects for the three-state subspace as obtained for the  $\text{H} + \text{H}_2$  system. Recently, we completed a detailed study of this system, and it was shown that increasing the nuclear region surrounding the  $D_{3h}$  ci, the two-state approximation soon breaks down so that the minimal Hilbert subspace has to be formed by three states.<sup>10a,b</sup> For the sake of completeness, we just add that continuing to increase this region leads slowly to the deterioration of the three-state subspace as well, and it soon becomes clear that at least five states are required etc.<sup>10c</sup> The present study concentrates on  $\tau_{13}$  or, to be more precise, on Curl  $\tau_{13}$  as given in eq 19c.

To carry out the proposed numerical treatment, we first have to reveal the positions of the ci's. Our way of doing that<sup>5,10,11</sup> is somewhat different from the “orthodox” way.<sup>23</sup> Namely, we fix the distance between two atoms and use the third atom as a test particle to locate ci's. The search is done in a given plane, and therefore the relevant coordinates are the planar coordinates of this atom. For reason of convenience, we choose the polar coordinates  $(q, \varphi)$ , and the results related to the various NACTs are presented in terms of these coordinates. The calculations are done along circles that are fixed by assigning the position of their centers and their radii  $q$ . As a result, the various calculated  $\tau$  matrix elements are presented as a function of  $\varphi$  ( $=\{0, 2\pi\}$ ) for fixed  $q$  values. As an example for the application of eq 17, we show in Figure 1 the vector analysis for the case of a system of two ci's. The positions of the ci's are marked by filled diamonds, i.e.,  $\blacklozenge$ , and the position of the center of the circle along which the calculations have to be done is marked by a filled circle, i.e.,  $\bullet$ . We also present small circles with radii  $\tilde{q}_j$  around each of the ci's: Along these circles are

calculated the respective ab initio virgin distributions  $f_j(\varphi_j)$  [ $=\tau_{\varphi}(\tilde{q}_j \sim 0, \varphi_j)$ ] to be employed in eq 17.

Finally, we make the following comments: No details are given regarding the ab initio calculations. They were presented in the appropriate papers (see ref 10 for  $\text{H} + \text{H}_2$  and ref 11 for  $\text{Na} + \text{H}_2$ ).

#### III.1. Numerical Studies of Two-State Systems. III.1.1.

**$\text{H} + \text{H}_2$  System.** We concentrate on configurations for which the distance,  $R_{\text{HH}}$ , between two hydrogens is fixed to be  $R_{\text{HH}} = 0.74 \text{ \AA}$  and allow the third hydrogen to be free. For these configurations, the  $\text{H}_3$  system is characterized by two important features: it possesses an equilateral ci known as the  $D_{3h}$  ci, which couples its two lower states, namely,  $1^2A'$  and  $2^2A'$ , and therefore is assigned as (1,2)  $D_{3h}$  ci, and two isosceles ci's, which couple the second and third states, namely,  $2^2A'$  and  $3^2A'$ , the two upper states. These two ci's were shown to be  $C_{2v}$  ci's and therefore are labeled as (2,3)  $C_{2v}$  ci's.

Because the  $\text{H}_3$  system lacks (3,4) ci's,<sup>10c</sup> the Hilbert subspace of three states covers a relatively extensive region in the configuration space around the (1,2)  $D_{3h}$  ci. As for the possibility of forming two-state Hilbert subspaces, it was shown that the lower two-state subspace is damaged significantly by the two upper (2,3) ci's.<sup>10a,b</sup> On the other hand, the upper two states can be shown to form a subspace upon a much more extensive region. This subspace is, indeed, perturbed by the lower (1,2)  $D_{3h}$  ci but only within a relatively small region around the (1,2)  $D_{3h}$  ci. Thus, for our purposes, the two upper states of the  $\text{H}_3$  system can be considered, approximately, as a two-state Hilbert subspace in a region that excludes (1,2)  $D_{3h}$  ci (and its close vicinity).

There is not much interest in showing the vector–algebra approach for the two lower states (in a small region around the  $D_{3h}$  ci) because these two states form only one ci. Still, our approach implies, based on previous studies, that  $\tau_{\varphi 12}(q, \varphi) \sim 0.5$  just like the value  $\tau_{\varphi 12}(q \sim 0, \varphi) \sim 0.5$ <sup>4a,6,7,10</sup> (we remind the reader that by  $\tau_{\varphi}$  we mean the angular component of  $\tau$  multiplied by  $q$ ). The deviations are at most  $\pm 10\%$  as long as we are not too close to the two (2,3) ci's (see Figure 2). In case the circle surrounds the (2,3) ci's, this approximation fails along a relatively large angular interval, where  $\tau_{\varphi 12}$  changes sign and becomes negative.

The upper subspace is, of course, much more interesting mainly because we encounter here two ci's, and this presents an interesting challenge for the vector–algebra approach.

In Figure 3 is given the virgin distribution  $f_{23}(\varphi_{23})$  ( $=\tau_{\varphi 23}(\tilde{q}_{23} \sim 0, \varphi_{23})$ ), as calculated for  $\tilde{q}_{23} = 0.02 \text{ \AA}$  (see also ref 10). Having these two  $f_{23}(\varphi_{23})$  functions, we are now in position to calculate the resulting molecular field. In Figure 4 are presented the results along the three circles centered at the (1,2) ci (we could, of course, choose any other circles or other contours) as shown by the schematic picture at the top of each column. It is important to emphasize that in these figures are presented the two components of  $\tau_{23}(q, \varphi)$ , namely,  $\tau_{\varphi 23}(q, \varphi)$  and  $\tau_{q 23}(q, \varphi)$ .

As is noticed, a very encouraging fit is obtained, and the rest is told by the results themselves. Still, we want to mention again that even the slight deviations are not necessarily due to the inadequacy of the vector–algebra but could be attributed to the background noise produced mainly by the (1,2) ci. For instance, the largest deviations are obtained along the circle with  $q = 0.2 \text{ \AA}$ , and this is because the (1,2) ci forces  $\tau_{23}(q, \varphi)$  to be zero at the (1,2) ci point—the location of the center of the circle—whereas the unperturbed  $\tau_{23}(q, \varphi)$  is, undoubtedly, dif-

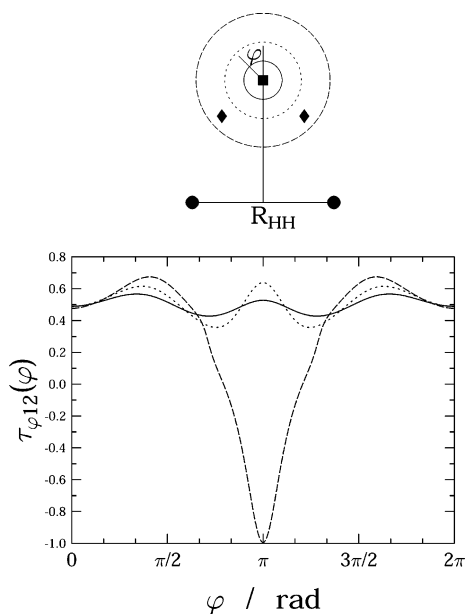


**Figure 2.** Ab initio angular component  $\tau_{\varphi 12}(\varphi|q=q_0)$  as a function of  $\varphi$  as calculated for the  $\text{H}_3$  system, for  $R_{\text{HH}} = 0.74 \text{ \AA}$ , along three circles centered at the (1,2)  $D_{3h}$  ci. The circles designate the two fixed hydrogens, the square designates the (1,2)  $D_{3h}$  ci, the diamonds designate the two symmetrical (2,3)  $C_{2v}$  ci's, and the straight line perpendicular to the HH axis connects the midpoint between the two hydrogens and the  $D_{3h}$  ci point. The full line is for  $q_0 = 0.1 \text{ \AA}$ , the dotted line is for  $q_0 = 0.2 \text{ \AA}$ , and the dashed line is for  $q_0 = 0.35 \text{ \AA}$ . It is noted that the values of  $\tau_{\varphi 12}(\varphi|q_0=0.1 \text{ \AA})$  are close to 0.5 and the values of  $\tau_{\varphi 12}(\varphi|q_0=0.35 \text{ \AA})$  are significantly different from those with  $q_0 = 0.1$  and  $0.2 \text{ \AA}$ .

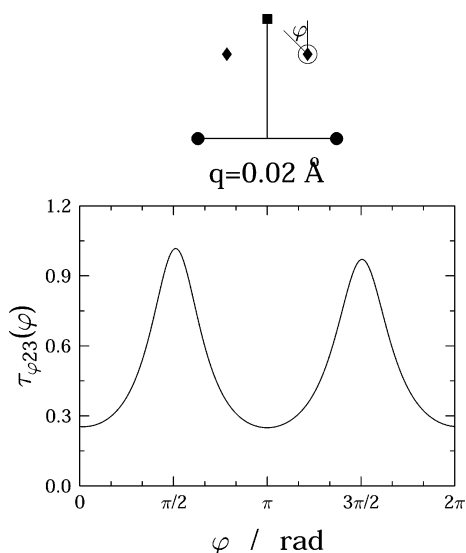


**Figure 3.** Ab initio angular component  $\tau_{\varphi 23}(\varphi|q_{23}=0.02 \text{ \AA})$  as calculated for the  $\text{H}_3$  system, for  $R_{\text{HH}} = 0.74 \text{ \AA}$ , along a circle of radius  $q_{23} = 0.02 \text{ \AA}$ . The circle surrounding the (2,3) ci is the circular contour along which  $\tau_{\varphi 23}(\varphi|q_{23})$  is calculated. The presented ci, together with the other symmetric ci, serves as the (2,3) *virgin* distribution to form the full (2,3) molecular field.

ferent from zero at this point. The effect of this (1,2) ci diminishes as the radius  $q$  increases.

**III.1.2. Na +  $\text{H}_2$  System.** We recently completed an extensive study of this system<sup>11</sup> and found two features that allow us to test our two-state vector–algebra approach for a much more complicated situation.

Within this study, the four lowest states of this system, namely,  $1^2A'$ ,  $2^2A'$ ,  $3^2A'$ , and  $4^2A'$ , were treated numerically.

For this purpose, we concentrated on configurations for which the distance,  $R_{\text{HH}}$ , between the two hydrogens, is fixed, namely,  $R_{\text{HH}} = 2.18 \text{ au}$ , and allowed the sodium to be free and serve as the test particle. The main findings for our present purpose are that the third and fourth states form a quasi two-state Hilbert subspace coupled by *four* (3,4) ci's. In other words, this system furnishes a unique opportunity to apply vector–algebra for a relatively complicated system with four sources (singularities).

The four ci's and the various circles along which the calculations were done are presented in Figure 5a,b. Out of these four ci's, two of them are  $C_{2v}$  ci's located on the symmetry line orthogonal to the HH axis at distances of  $r \sim 1.580 \text{ au}$  and  $1.145 \text{ au}$  from the HH axis (they are designated as *top* and *bottom* ci's, respectively) and two *twin*  $C_s$  ci's located on both sides of the just mentioned symmetry line at a distance of  $r = 1.533 \text{ au}$  from the HH axis and at an angle of  $12.2^\circ$  off this, symmetry, line (they are designated as *sideward* ci's).

The *virgin* distributions,  $f_j(\varphi_j)$ , for three ci's, namely, for the top ci, the bottom ci, and one of the sideward ci's, are shown in Figure 6. It is noticed that all of them are of the elliptic type<sup>24a</sup> (in contrast to the circular Jahn–Teller type<sup>24b</sup>). These virgin distributions are interesting by themselves. For instance, the two ci's on the symmetry line behave essentially orthogonal to each other; namely, the main distribution of the top ci is parallel to the HH axis, whereas the main distribution of the bottom ci is along the symmetry line. The distributions of the sideward ci's are somewhat different. They are of the elliptic kind, but their main distribution is not along the line parallel to the HH axis (nor along the symmetry line) but along a line that is rotated by about  $10^\circ$  from the HH axis.

We return again to Figure 5 to discuss the various circles along which the calculations were performed. In Figure 5a are given three circles with their centers at the origin  $\mathbf{O}(0,0)$  (defined as the crossing point between the symmetry line and a line parallel to the HH axis that passes through the two sideward ci's) and with radii  $q = 0.16, 0.30$ , and  $0.40 \text{ au}$ . Figure 5b presents a similar situation, but this time the center of the one presented circle, with the radius  $q = 0.25 \text{ au}$ , is shifted, from the origin  $\mathbf{O}(0,0)$  downward by  $0.135 \text{ au}$ . In this way, we could get results for a circle that surrounds only the two ci's located on the symmetry line.

The model results and the ab initio ones are compared in Figure 7. In fact, like in the previous  $\text{H}_3$  system, the results speak for themselves. It is noticed that, although the ab initio distributions are frequently quite complicated and show a lot of structure, the vector–algebra approach produces functions that are capable of following very accurately the ab initio wiggles.

**III.2. Numerical Studies of the Three-State System.** The study of the three-state system is not as extensive as that of the previous two-state system for two reasons: (a) We only have one system available that presents truly three coupled states, namely, the  $\text{H} + \text{H}_2$  system (for  $\text{Na} + \text{H}_2$ , we found that any two-state system is only weakly coupled to a third state). (b) Even for the one available system, we present only a few results because the full study is not completed yet.

The magnitude that most characterizes a three-state system is  $\tau_{13}(q, \varphi)$  for the simple reason that if  $\tau_{13}(q, \varphi)$  is identically zero, the three-state subspace breaks up into two two-state subspaces (as discussed earlier). We also recall that  $\tau_{13}(q, \varphi)$  is formed as a result of the mutual interaction between  $\tau_{12}(q, \varphi)$  and  $\tau_{23}(q, \varphi)$  (see eq 19c). It is important to realize that if this mutual interaction is zero (it happens when the two functions

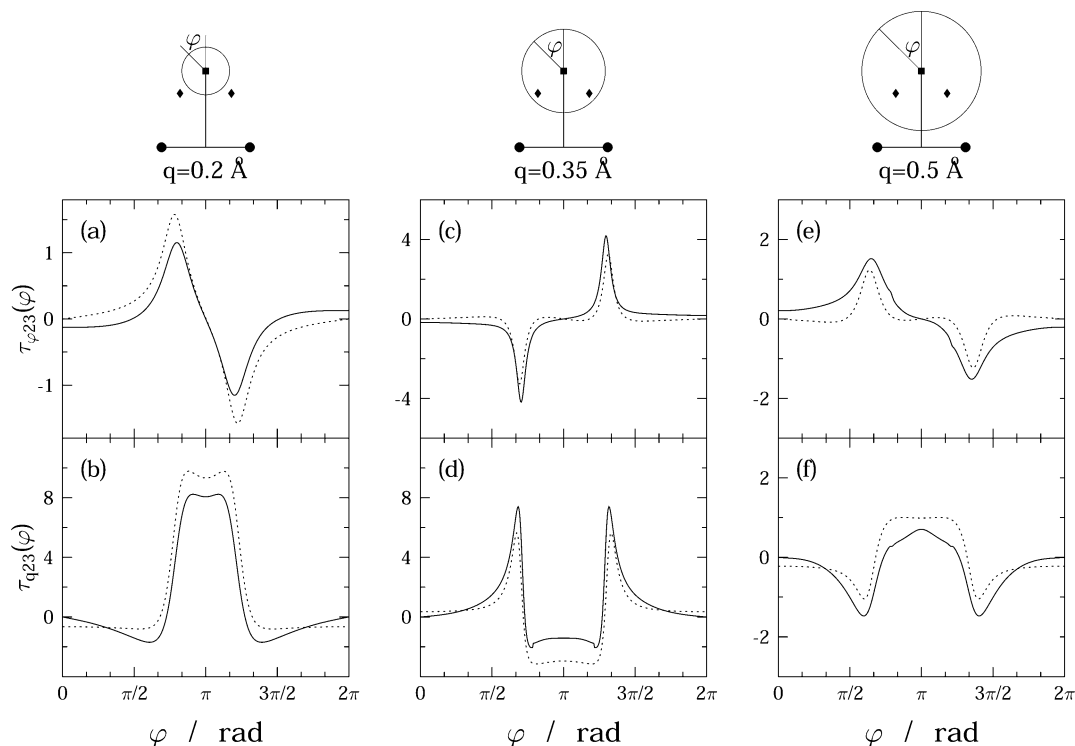


**Figure 4.** Final results for the  $\text{H} + \text{H}_2$  system: A comparison between ab initio and vector–algebra results for the  $\tau_{23}(\varphi|q)$  NACT as calculated along two circles centered at the  $D_{3h}$  ci (the schematic picture of each circle is given at the top of the relevant column). In parts a, c, and e are presented the angular components  $\tau_{\varphi 23}(\varphi|q)$ , and in parts b, d, and f are presented the radial components,  $\tau_{q 23}(\varphi|q)$ . Full lines are ab initio calculations; dashed lines are vector–algebra calculations.

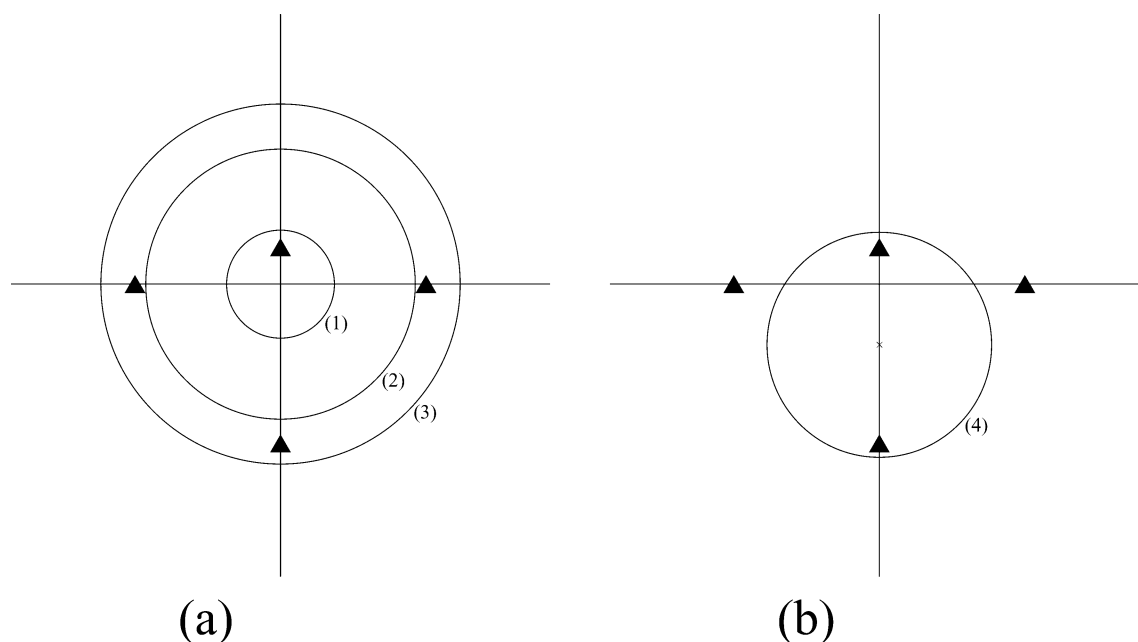


**Figure 5.** Four (3,4) conical intersections of the  $\text{Na} + \text{H}_2$  system: (a) three concentric circles with their centers at  $\mathbf{O}(0,0)$  surrounding different numbers of conical intersections; (b) a circle with its center at  $\mathbf{O}(0, -0.135)$  surrounding the two conical intersections located on the symmetry line.

$\tau_{12}(q, \varphi)$  and  $\tau_{23}(q, \varphi)$  do not overlap),  $\tau_{13}$  becomes zero, although according to eq 19c only Curl of  $\tau_{13}$  (and not  $\tau_{13}$ ) becomes zero. Still, because  $\tau_{13}$  does not have a source of its own, the fact that Curl  $\tau_{13} = 0$  implies that  $\tau_{13} = 0$ .

The subject we intend to study here is related to eq 19c. We discuss two issues: (1) Having the ab initio  $\tau_{12}(q, \varphi)$  and  $\tau_{23}(q, \varphi)$ , it will be shown that their vector product, indeed, forms Curl  $\tau_{13}$ . (2) The same treatment is repeated by employing  $\tau_{12}(q, \varphi)$  and  $\tau_{23}(q, \varphi)$  as obtained from the vector–algebra; namely, we intend to show that approximately Curl  $\tau_{13}$  can also

be formed by vector–algebra as applied to the  $\text{H}_3$ -virgin distributions  $f_{12}(\varphi_{12})$  and  $f_{23}(\varphi_{23})$ .

We start with the first issue, and for this sake, we derive each side of eq 19c independently. The left-hand side, namely, the Curl itself, is calculated in two steps: first are derived the two components of  $\tau_{13}(q, \varphi)$  (see eq 3) by employing MOLPRO and, second, are calculated numerically the  $q$  and  $\varphi$  derivatives of  $\tau_{13\varphi}(q, \varphi)$  and  $\tau_{13q}(q, \varphi)$ , respectively, to form the required Curl function. The right-hand side is obtained by employing the ab initio components of  $\tau_{12}(q, \varphi)$  and  $\tau_{23}(q, \varphi)$  as calculated

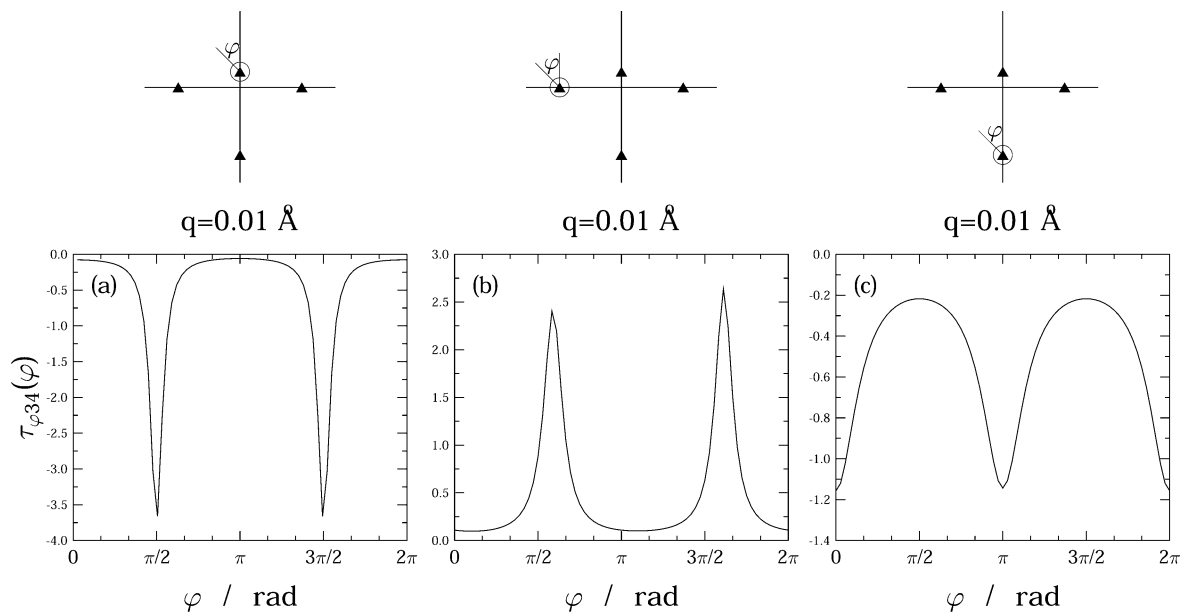


**Figure 6.** Three ab initio angular components  $\tau_{\phi 34}(\phi|q_{34}=0.01 \text{ au})$  as calculated for the Na + H<sub>2</sub> system for  $R_{\text{HH}} = 2.18 \text{ au}$ : (a)  $\tau_{\phi 34}(\phi|q_{34}=0.01 \text{ au})$  calculated for the upper (3,4) ci on the symmetry line; (b)  $\tau_{\phi 34}(\phi|q_{34}=0.01 \text{ au})$  calculated for the sideward (3,4) ci; (c)  $\tau_{\phi 34}(\phi|q_{34}=0.01 \text{ au})$  calculated for the lower (3,4) ci on the symmetry line. The three presented curves, together with the second sideward ci, serve as the four (3,4) virgin distributions to form the full (3,4) molecular field.

by MOLPRO and forming the relevant vector products. The calculations were carried out along circles with different radii  $q$  that have their centers at the (1,2)  $D_{3h}$  ci. To have results for a series of different radii is important because of the strong effect furnished by the two (2,3)  $C_{2v}$  ci's (see Figure 2) on  $\tau_{12}(q, \phi)$ .

The results of these two different calculations are presented and compared in parts a and c of Figure 8 for circles with two different radii, i.e.,  $q = 0.20$  and  $0.35 \text{ Å}$ , respectively. It is noticed that for all practical purposes the two different calculations yield the same results.

To carry out the study of the second case, we employ, as mentioned earlier, values obtained from the virgin distributions and vector-algebra. Thus, the left-hand side of eq 19c is calculated as before, and only the right-hand side is produced differently, employing magnitudes that follow from vector-algebra. For this purpose, we need the values of  $\tau_{12}$  and  $\tau_{23}$ . It is important to emphasize that this procedure is expected to succeed at situations where the components of  $\tau_{12}$  and  $\tau_{23}$  are not damaged too much by each other, an assumption that is only in part fulfilled for the H<sub>3</sub> system.

We discussed extensively the required values of  $\tau_{23}$  (also shown in Figure 4) and only to a limited extent the values of  $\tau_{12}$ . So now we extend somewhat our considerations concerning  $\tau_{12}$ . From previous studies, we know that the virgin shape of  $\tau_{\phi 12}(\phi|q)$  is on average a constant, namely,  $f_{12}(\phi_{12}) = 0.5$ ,<sup>4a,6,7,10</sup> and it holds as long as the circle around the (1,2)  $D_{3h}$  ci is not too close to the (2,3) ci's and does not surround them.<sup>10</sup> In Figure 2 is presented  $\tau_{\phi 12}(\phi|q)$  as a function of  $\phi$  for three different values of  $q$ . It is noticed that the basic assumption regarding  $\tau_{\phi 12} \sim 0.5$  is fulfilled as long as the just mentioned conditions are met (see how dramatically  $\tau_{\phi 12}$  is changed for the case of  $q = 0.35 \text{ Å}$ ). As for the radial component, on the basis of ab initio calculations, it is known to be not only relatively small<sup>11b</sup> (in particular, as compared to  $\tau_{\phi 12}/q$ ) but also oscillating around zero, and therefore we assume it, throughout the numerical treatment, to be zero, i.e.,  $\tau_{q12}(\phi|q) \equiv 0$ .

Once having the *unperturbed* components of  $\tau_{12}$  and  $\tau_{23}$ , the right-hand side of eq 19c can be obtained as in the previous case. Calculations were done for the previously mentioned two

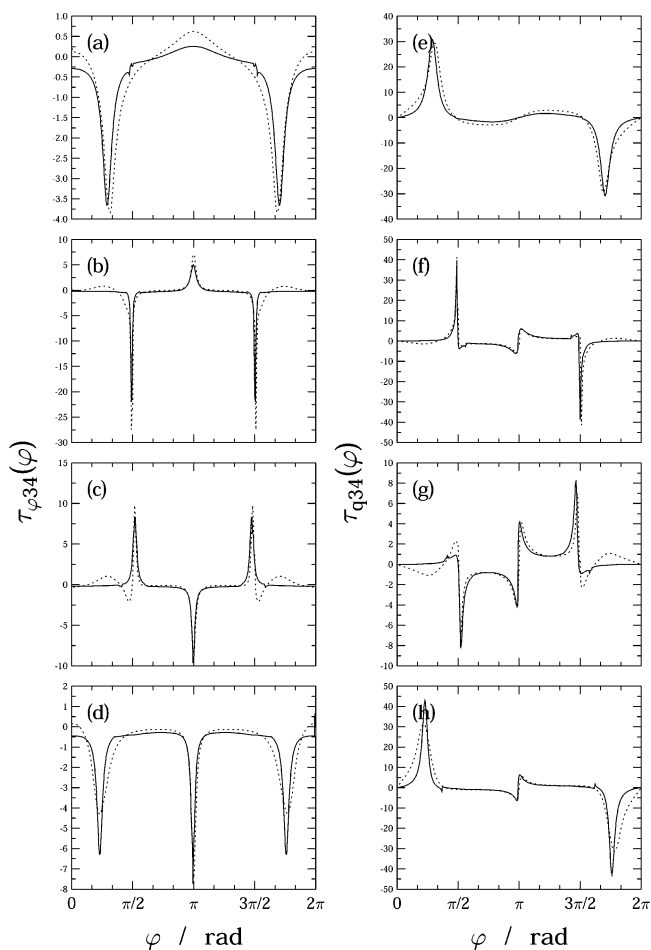


**Figure 7.** Final results for the Na + H<sub>2</sub> system: A comparison between ab initio and model results for the  $\tau_{34}(\phi|q)$  NACT as calculated along four circles presented in Figure 5. In parts a, c, e, and g are presented the angular components,  $\tau_{\phi 34}(\phi|q)$ , and in parts b, d, f, and h are presented the radial components,  $\tau_{q 34}(\phi|q)$ . Full lines are the results due to ab initio calculations; dashed lines are the results due to vector-algebra calculations.



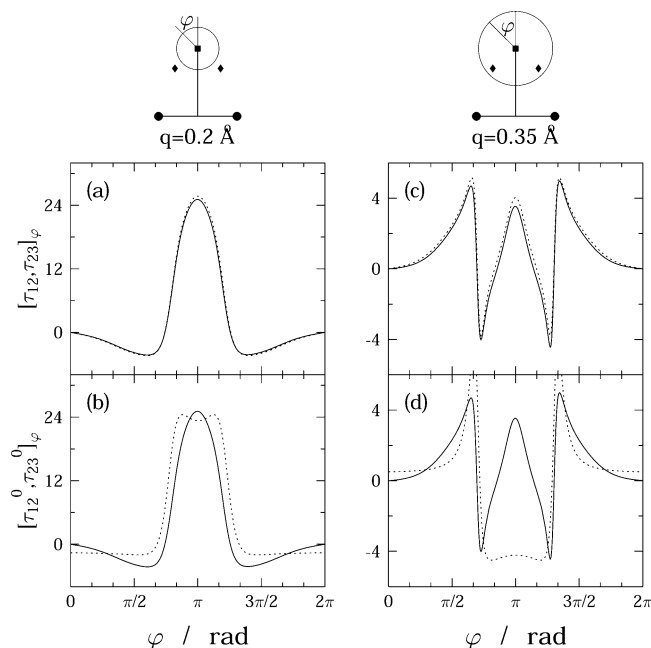


**Figure 8.** Results for the  $\text{H} + \text{H}_2$  system as calculated for the two circles centered at the  $D_{3h}$  ci. In parts a and b are presented the results for Curl  $\tau_{13}(q|q=0.2 \text{ \AA})$ , and in parts c and d are presented the results for Curl  $\tau_{13}(q|q=0.35 \text{ \AA})$ . Full lines present the results due to the left-hand side of eq 19c (mentioned also as the Maxwellian Curl), and dotted lines present the results due to the right-hand side of eq 19c, namely, the vectorial product. In parts a and c, the vectorial product is formed from magnitudes formed by ab initio calculations, and in parts b and d, the vectorial product is formed from magnitudes obtained by vector-algebra calculations.

circles, and the results are presented in Figure 8b,d, where they are compared again with those obtained by the Curl expression on the left-hand side of eq 19c. A reasonable good fit is obtained for the smaller  $q$  value, where the circle is relatively far both from the two (2,3) ci's and from the center where the (1,2)  $D_{3h}$  ci is located (see Figure 8c). In other words, it is seen that the unperturbed (1,2) and (2,3) NACTs are, indeed, responsible for the (1,3) Curl equation. A somewhat less satisfying fit is obtained for the circle with the larger radius, namely,  $q = 0.35 \text{ \AA}$  (see Figure 8d). Whereas a reasonable agreement is achieved as long as  $\varphi$  is outside the angular interval  $\varphi = [135^\circ, 225^\circ]$ , it fails along this interval. The reason is directly associated with the assumption that  $\tau_{\varphi 12}(q|\varphi) \sim 0.5$  for any  $q$  and  $\varphi$ . From Figure 2, it is seen that when the circle surrounds also the (2,3) ci's, this assumption breaks down, in particular, along the above-mentioned angular range because of the strong interaction between  $\tau_{\varphi 12}$  and  $\tau_{\varphi 23}$ . More about this subject and how to correct for this mishap will be discussed elsewhere.

#### IV. Conclusions

This paper belongs to a group of papers<sup>1,2,15,21,22</sup> that are devoted to the idea that the components of the NACTs behave like a (Maxwellian) vector potential and as a result their features can be derived by solving the relevant electrodynamics equations. According to our approach, the field created by the NACTs, which we termed the *molecular field*, has its source(s) at the degeneracy points, namely, at the points of the ci's. We considered two types of NACTs: two-state NACTs that are formed by a two-state Hilbert subspace and three-state NACTs that are formed by a three-state Hilbert subspace. For the two-state NACTs, the relevant Curl equation is zero (except at the source points), and therefore their spatial distribution, according

to our approach, follows from straightforward application of vector-algebra. The situation, in the case of three-state NACTs, is much more complicated: It is not only that the relevant Curl equations are not homogeneous (see eqs 19), but we have to consider three such equations (instead of two): two equations for  $\tau_{12}$  and  $\tau_{23}$ , which are formed by sources connected to degeneracy between adjacent states, and one for  $\tau_{13}$ , which lacks a source and results from the interaction between  $\tau_{12}$  and  $\tau_{23}$ , as is evident from eq 19c. In the present paper, we just refer to  $\tau_{13}$  and study the behavior of its Curl equation.

The numerical study is carried out by comparing the ab initio results obtained from MOLPRO with the results that follow from the vector-algebra based on the angular NACTs calculated (by MOLPRO) in the close vicinity of the relevant ci's. These types of angular NACTs are termed as *virgin* NACTs because very close to their own ci's all NACTs are basically pure two-state NACTs (immaterial how many ci's are in its vicinity). The vector-algebra that is applied is described in Figure 1 and explicitly presented in eqs 16 and 17.

To perform this study, we considered two systems, namely,  $\text{H} + \text{H}_2$  and  $\text{Na} + \text{H}_2$ . The two-state study was done for the two ci's formed by the second and third states of the  $\text{H} + \text{H}_2$  system and the four ci's formed by the third and fourth states of the  $\text{Na} + \text{H}_2$  system. The three-state study was done for the three states of the  $\text{H} + \text{H}_2$  system, whereas within the two-state study, the relevant molecular fields  $\tau_{23}$  of  $\text{H} + \text{H}_2$  and  $\tau_{34}$  of  $\text{Na} + \text{H}_2$  were calculated directly (by applying vector-algebra); in the case of the three-state study, we derived Curl  $\tau_{13}$  (and not  $\tau_{13}$  itself) but again employing vector-algebra as dictated by eq 19c.

The comparison between the ab initio calculations and the analytical results undoubtedly indicates that, indeed, the *molecular fields* are created by sources located at the degeneracy points formed by the Born–Oppenheimer adiabatic states.

This finding has a very important implication on what the NACTs really are. The NACTs were always considered as coupling terms with *random* values something of the kind that are reminiscent of potential energy surfaces. Now we see that in the case of NACTs they are governed by very basic laws of physics, and in fact all we have to know is the location of the ci's in a given region and the corresponding *virgin* distributions; the rest are Maxwell equations, which in the present two-state case are “solved” by employing vector-algebra.

The treatment in this paper is applicable for planar geometries. Although it looks as if the planar geometry is far from the general case, our point of view is that the general case can be presented in terms of a series of parallel planes that are close enough to each other but any plane can, still, be treated independently.

Before concluding this paper, we refer briefly to one assumption that enabled the construction of this model, namely, that ci's seem to produce small enough radial components of  $\tau$ , namely,  $\tau_q$ , that eq 14 (in particular, the last part of it) is approximately valid. It could very well be that  $\tau_q$  is not really that small, but the fact that the model was able to produce these kinds of results implies that  $\tau_q$  is not large enough to ruin its successful application.

**Acknowledgment.** A.V. and M.B. acknowledge the OTKA grant (T037994) and the Szent-Györgyi Albert grant for supporting this research. M.B. also thanks A.V. for her warm hospitality during his stay at the Department of Physics, University of Debrecen.

## References and Notes

- (1) Avery, J.; Baer, M.; Billing, G. D. *Mol. Phys.* **2002**, *100*, 1011.
- (2) Baer, M.; Mebel, A. M.; Billing, G. D. *Int. J. Quantum Chem.* **2002**, *90*, 1577.
- (3) Baer, M.; Billing, G. D. The Role of Degenerate States in Chemistry. *Adv. Chem. Phys.* **2002**, *124*.
- (4) Yarkony, D. R. *J. Chem. Phys.* **1996**, *105*, 10456.
- (5) Mebel, A. M.; Baer, M.; Lin, S. H. *J. Chem. Phys.* **2000**, *112*, 10703. Mebel, A. M.; Baer, M.; Rozenbaum, V. M.; Lin, S. H. *Chem. Phys. Lett.* **2001**, *336*, 135. Mebel, A. M.; Halasz, G. J.; Vibok, A.; Alijha, A.; Baer, M. *J. Chem. Phys.* **2002**, *117*, 991.
- (6) Abrol, R.; Kuppermann, A. *J. Chem. Phys.* **2002**, *116*, 1035.
- (7) Kuppermann, A.; Abrol, R. *Adv. Chem. Phys.* **2002**, *124*, 283.
- (8) Englman, R.; Yahalom, A. *Adv. Chem. Phys.* **2002**, *124*, 197.
- (9) Child, M. S. *Adv. Chem. Phys.* **2002**, *124*, 1.
- (10) (a) Halasz, G. J.; Vibok, A.; Mebel, A. M.; Baer, M. *J. Chem. Phys.* **2003**, *118*, 3052. (b) Halasz, G. J.; Vibok, A.; Mebel, A. M.; Baer, M. *Chem. Phys. Lett.* **2002**, *358*, 163. (c) Baer, M.; Vertesi, T.; Halasz, G. J.; Vibok, A.; Suhai, S. *Faraday Discuss.* **2004**, *127*, in press.
- (11) Vibok, A.; Halasz, G. J.; Vertesi, T.; Suhai, S.; Baer, M.; Toennies, J. P. *J. Chem. Phys.* **2003**, *119*, 6588.
- (12) Born, M.; Oppenheimer, J. R. *Ann. Phys. (Leipzig)* **1927**, *84*, 457. Born, M. *Gott. Nachr. Math. Phys.* **1951**, *Kl.*, 1.
- (13) Baer, M. *Chem. Phys. Lett.* **1975**, *35*, 112.
- (14) Hellmann, H. *Einführung in die Quantenchemie*; Franz Deutiche: Leipzig, 1937. Feynman, R. *Phys. Rev.* **1939**, *56*, 340.
- (15) Baer, M. *Chem. Phys. Lett.* **2001**, *349*, 84.
- (16) Englman, R. *The Jahn–Teller Effect in Molecules and Crystals*; Wiley-Interscience: New York, 1972.
- (17) Bersuker, I. B. *Chem. Rev.* **2001**, *101*, 1067. Bersuker, I. B.; Polinger, V. Z. *Vibronic Interactions in Molecules and Crystals*; Springer: New York, 1989.
- (18) (a) Baer, M. *Chem. Phys. Lett.* **2000**, *329*, 450. (b) Baer, M.; Englman, R. *Chem. Phys. Lett.* **2001**, *335*, 85.
- (19) Kryachko, E. S. *Adv. Quantum Chem.* **2003**, *44*, 119. Koppel, H. *Faraday Discuss.* **2004**, *127*, in press. Rebentrost, F. In *Theoretical Chemistry: Advances and Perspectives*; Henderson, D., Eyring, H., Eds.; Academic Press: New York, 1981; Vol. II, p 32. Mead, C. A.; Truhlar, D. G. *J. Chem. Phys.* **1982**, *77*, 6090. Chapuisat, X.; Nauts, A.; Dehareug-Dao, D. *Chem. Phys. Lett.* **1983**, *95*, 139. Petrongolo, C.; Hirsch, G.; Buenker, R. *Mol. Phys.* **1990**, *70*, 825, 835. Sidis, V. *Adv. Chem. Phys.* **1992**, *82* (Vol. II), 73. Vertesi, T.; Vibok, A.; Halasz, G. J.; Yahalom, A.; Englman, R.; Baer, M. *J. Phys. Chem. A* **2003**, *107*, 7189. Pacher, T.; Cederbaum, L. S.; Köppel, H. *Adv. Chem. Phys.* **1993**, *84*, 293.
- (20) Baer, M.; Alijah, A. *Chem. Phys. Lett.* **2000**, *319*, 489. Baer, M.; Lin, S. H.; Alijah, A.; Adhikari, S.; Billing, G. D. *Phys. Rev. A* **2000**, *62*, 032506-1. (b) Adhikari, S.; Billing, G. D.; Alijah, A.; Lin, S. H.; Baer, M. *Phys. Rev. A* **2000**, *62*, 032507-1.
- (21) Hu, S.; Halasz, G. J.; Vibok, A.; Mebel, A. M.; Baer, M. *Chem. Phys. Lett.* **2003**, *367*, 177.
- (22) Baer, M. *Chem. Phys. Lett.* **2002**, *360*, 243.
- (23) Longuet-Higgins, H. C. *Proc. R. Soc. London, Ser. A* **1975**, *344*, 147.
- (24) (a) Baer, M.; Mebel, A. M.; Englman, R. *Chem. Phys. Lett.* **2002**, *354*, 243. (b) Baer, M.; Englman, R. *Mol. Phys.* **1992**, *75*, 283.